

# Effects of different substrate on the structural and optical properties of atomic layer deposited TiO<sub>2</sub> thin films

SYED MANSOOR ALI<sup>a\*</sup>, S.A. AL SALMAN<sup>a</sup>, S.S. AL-GHAMDI<sup>a</sup>, M. S. AL GARAWI<sup>a</sup>, M. R. BAIG<sup>a</sup>,  
TURKI S. ALKHURAJI<sup>b</sup>

<sup>a</sup>*Department of Physics and Astronomy, College of Science, P.O BOX 2455 King Saud University Riyadh 11451 Saudi Arabia*

<sup>b</sup>*National Center for Irradiation Technology, King Abdulaziz City for Science & Technology, Saudi Arabia*

In this work, Titanium dioxide (TiO<sub>2</sub>) thin films were prepared by atomic layer deposition (ALD). The effect of different substrates on the structural and optical properties of TiO<sub>2</sub> thin films was studied. The prepared films were characterized by X – Ray diffraction (XRD) method, reflectance spectroscopy, Photoluminescence (PL) spectroscopy, Field Effect Scanning Electron Microscopy (FESEM) and Energy Dispersive X – Ray (EDX). The XRD results show that the anatase and rutile mixed crystalline TiO<sub>2</sub> structure for each substrate. The stoichiometric ratio of the film was confirmed by EDX analysis. The room temperature PL spectra of TiO<sub>2</sub> thin films show the band gap and defect peak at 409 nm and 420 nm with excitation at 325 nm. The surface morphology shows that TiO<sub>2</sub> on FTO have high roughness as compared to others with irregular particles.

(Received November 30, 2015; accepted August 3, 2016)

**Keywords:** Atomic layer deposition, XRD, FESEM, Photoluminescence, Refractive index

## 1. Introduction

Material preparation technology plays an important role on physical and surface chemical properties of TiO<sub>2</sub>, which strongly depend on its electrical, structural, as well as optical properties [1]. Therefore, choice of a well-controllable technology to engineer the defects in TiO<sub>2</sub> is an important task for specific application. Among the variety of deposition techniques, atomic layer deposition (ALD) is a chemical method to grow uniform thin films in an atomically controlled composition, which allows for the conformality of complex structures with precise thickness and a high degree of purity [2]. The growth of TiO<sub>2</sub> thin films by ALD is a well known process and has been recently reviewed [3]. Transportation and separation of Charge carrier, which highly depend on interface and surface properties [4,5], are among the most important aspects of energy conversion processes.

Titanium dioxide (TiO<sub>2</sub>) is an important material in different applications for its large band gap [6], high refractive index [7,8], high dielectric constant [9,10], and highly active surface. Among various oxide semiconductor photocatalysts, titania is a very important photocatalyst for its strong oxidizing power, nontoxicity, and long-term photostability [11, 12]. TiO<sub>2</sub> is also promising material for degradation of organic molecules, such as purification of waste water [13], disinfection in public [14], self-cleaning

coating [15], corrosion-protection [16], and actively suppressed impact on tumor cells [17-19]. Further more, TiO<sub>2</sub> as a semiconducting metal oxide, can be used as oxygen gas sensor [20, 21] and metal oxide semiconductor field effect transistors (MOSFET) [22].

In this study, TiO<sub>2</sub> thin films were deposited on different substrates by ALD technique. The dependences of the surface morphology, refractive index, and crystal structure and defects of the TiO<sub>2</sub> thin films on the different substrate are investigated in details by field effect scanning electron microscope (FESEM), X-ray diffraction (XRD), photoluminescence (PL), and reflectance spectroscopy.

## 2. Experimental

In this work, TiO<sub>2</sub> thin films have been deposited on different substrate like p type Si (100) wafer, FTO and glass by atomic layer deposition at 200 C<sup>0</sup> substrate temperature and ~ 17 hPa pressure. The deposited TiO<sub>2</sub> thin films has been prepared from precursors TiCl<sub>4</sub> and deionized water enclosed in bottles which is kept at room temperature. The fabrication process of thin films consist of series of alternative cycles of precursors reactions on the substrate surface. Every cycle divided up further into two half cycles. In the first half cycle, TiCl<sub>4</sub> pulse carried out to the reaction chamber by carrier gas which is

nitrogen gas with (99.9999%) purity and self-terminating reactions occurs on the substrate. The residual, non-reacted reactant and byproduct are removed from the chamber by purging. In the next half cycle, pulse of deionized water is carried out to the reaction chamber by carrier gas which ends at self-terminating reaction and by product is purged out. The flow rate of the carrier gas at TiCl<sub>4</sub> and at deionized water line flow adjusted to 150 sccm and 200 sccm and pressure 9 hPa and 8 hPa, respectively. The pulsing scheme for the deposition of TiO<sub>2</sub> thin films carried out as TiCl<sub>4</sub>/N<sub>2</sub>/H<sub>2</sub>O/N<sub>2</sub> with pulsing time 0.1 s/3 s/ 0.1 s/ 4 s. The growth rate per cycle has measured to 0.4 Å<sup>0</sup>. The thin film of 100 nm thickness with very low roughness has been obtained by performing 2500 cycles.

The XRD analysis of TiO<sub>2</sub> thin films was carried out using multipurpose x-ray diffractometer (Bruker, D8 Discover) with CuK $\alpha$  source radiation. Surface morphology of the films was investigated with JEOL (JSM-7600F) Field Emission electron microscope. Optical reflectance studies were made at room temperature by using UV-Vis-NIR spectrophotometer (JASCO – V 670) in the wavelength range 200-800 nm. PL spectra of the TiO<sub>2</sub> thin films were measured at room temperature under the excitation of the 325-nm by spectrofluorometer (FP-8200).

### 3. Results and discussion

The XRD patterns of TiO<sub>2</sub> thin films deposited at 200°C onto different substrates by atomic layer deposition are shown in Fig. 1. The peaks in the spectra of TiO<sub>2</sub> thin films deposited on Si, glass and FTO substrates confirmed the mixed anatase and rutile structure by JCPDS 84-1286 and JCPDS 88-1175 respectively. The other peaks arise from the substrates as indicated in Fig. 1. However, in the cases of Si substrate one can not that the intensity of both anatase and rutile peaks of TiO<sub>2</sub> is higher and then gradually decrease for glass and FTO substrate respectively. Furthermore a small angular shift of the peaks is observed with changing substrates.

To attain the detailed structure information, the crystallite size D for anatase and rutile peaks of TiO<sub>2</sub> thin films was calculated according to the Scherrer equation (1) [23].

$$D = \frac{0.9\lambda}{\beta \cos \theta} \quad (1)$$

where D is the crystallite size,  $\lambda$  is the X-ray wavelength ( $\lambda = 1.5406 \text{ \AA}$ ),  $\beta$  is the full width at half-maximum (FWHM), and  $\theta$  is Bragg angle of peak. It was observed from XRD analysis that the crystallite size calculated by anatase peak is higher as compared to the rutile peaks for each substrate.

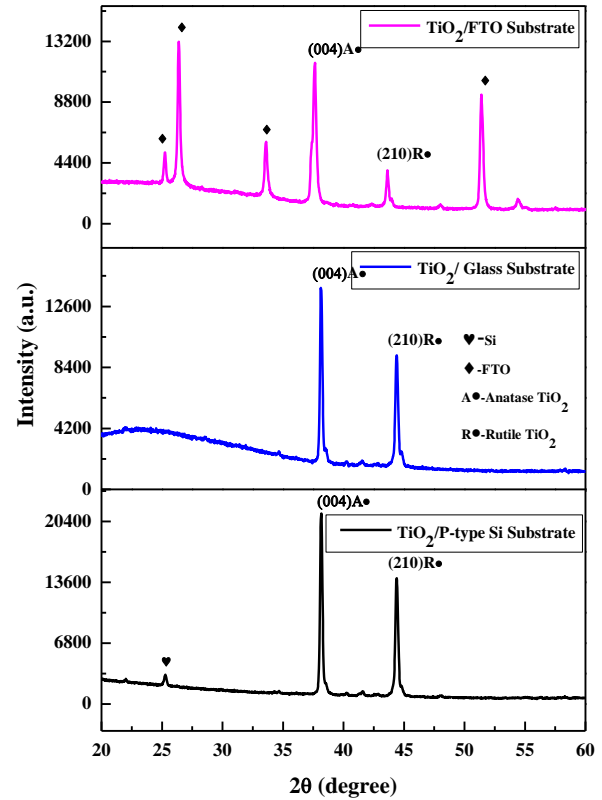


Fig. 1. XRD patterns of TiO<sub>2</sub> thin films on different substrates.

The strain in the TiO<sub>2</sub> thin films is related to the lattice misfit between the film and substrate, which in turn depends upon the deposition conditions. For same deposition condition the micro strain ( $\mu$ ) developed in the atomic layer deposition coated TiO<sub>2</sub> thin films was calculated from the equation (2) [24],

$$\mu = \frac{\beta \cos \theta}{4} \quad (2)$$

This type of micro strain changes may be due to the crystallization process in crystalline thin films of TiO<sub>2</sub>. The number of crystallites 'N' was calculated from equation (3) [25].

$$N = \frac{t}{D_3} \quad (3)$$

where 't' is the thickness of the film and 'D' is the crystallite size. The dislocation density ( $\delta$ ), defined as the length of dislocation lines per unit volume, are estimated using the equation (4) [26].

$$\delta = \frac{1}{D^2} \quad (4)$$

The calculated results from XRD are given in table1.

Table 1. XRD results of TiO<sub>2</sub> thin films on different substrate.

TiO <sub>2</sub> thin films		Positions (2θ)	FWHM (deg)	Crystallite size D (Å)	Microstrain $\mu \times 10^{-2}$	No. of crystallites $N \times 10^{21}$	Dislocation $\delta \times 10^{18}$ (lines/m <sup>2</sup> )
Si	Anatase	37.63	0.25	6.5	5.9	0.73	2.3
	Rutile	44.39	0.29	5.73	6.7	1.06	3.04
Glass	Anatase	38.09	0.27	6.03	6.3	0.91	2.75
	Rutile	44.34	0.29	5.73	6.68	1.06	3.04
FTO	Anatase	38.19	0.24	6.6	5.7	0.69	2.45
	Rutile	43.65	0.27	6.14	6.2	0.86	2.65

Fig. 2 shows SEM micrographs of the TiO<sub>2</sub> thin films deposited on different substrate Si (a), glass (b) and FTO (c). It can be observed that the surface morphologies and roughness of the TiO<sub>2</sub> thin films are different for different substrates. For Si substrate a dense nano films composed of TiO<sub>2</sub> nano crystals was formed as shown in Fig 2(a). The TiO<sub>2</sub> thin film on glass consists of spherical particles with a diameter ranging from 60 to 80 nm and they are agglomerate to each other clearly notice in Fig 2 (b). Fig 2 (c) the TiO<sub>2</sub> thin film suggests, the film is rough and looks more like a population of small and large particles. The particle size and its distribution are affected by changing of the substrate due to the small lattice mismatching between substrate and TiO<sub>2</sub>.

EDX technique was used to study the stoichiometry of the TiO<sub>2</sub> thin films. Fig. 3 (a, b and c) shows typical EDX patterns of the TiO<sub>2</sub> thin films on different Si, glass and FTO substrate respectively. The elemental analysis was carried out only for Ti and O. However, there are some additional peaks in the EDX spectra, which could be due to the presence of these elements in the substrates

Fig. 4 shows the reflectance 'R' of TiO<sub>2</sub> thin films on different substrate as function of wave length. The spectra show the interference pattern for Si and glass substrate have almost similar trend with slightly shift of peaks while for FTO substrate the spectrum is different as compared to Si and glass substrate. It may be due to the structure changes as observed in XRD.

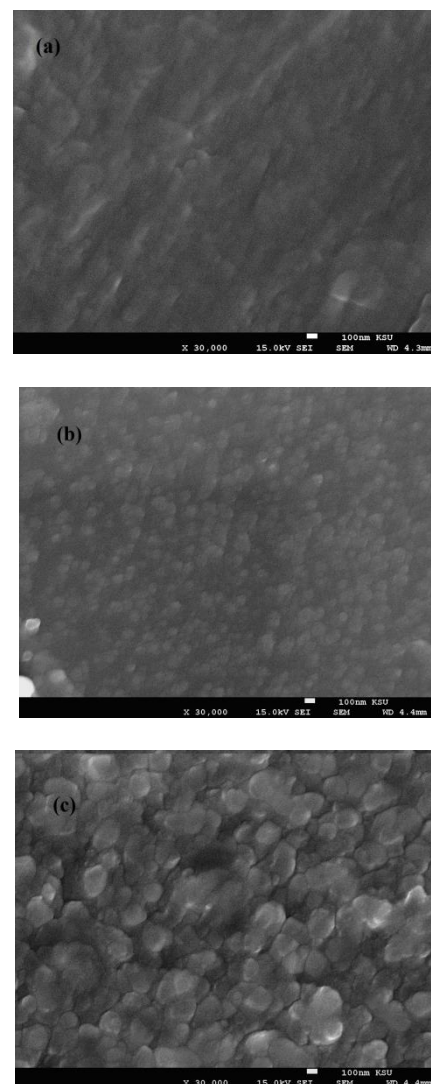


Fig. 2. FESEM images of TiO<sub>2</sub> thin films on (a) Si (b) glass and (c) FTO substrate.

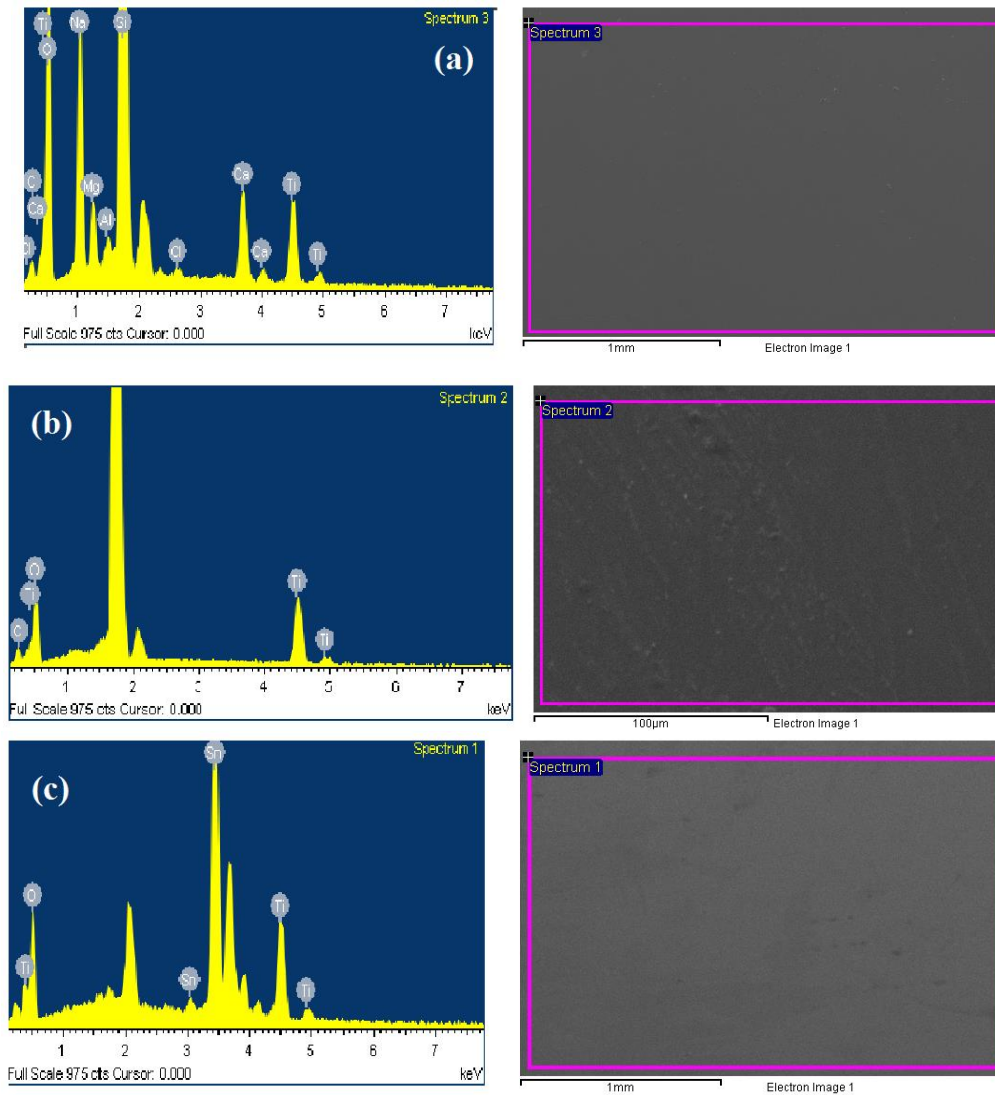


Fig. 3. EDX spectrum of TiO<sub>2</sub> thin films on (a) Si (b) glass and (c) FTO substrate.

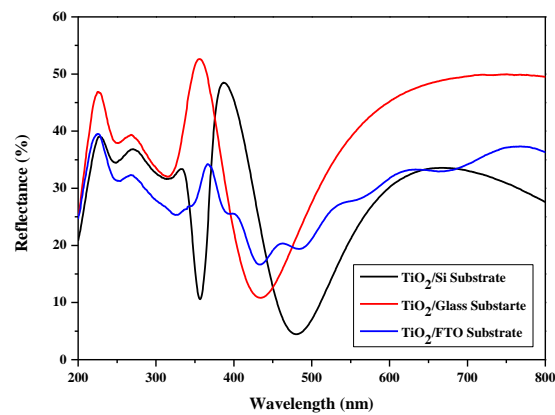


Fig. 4. Reflectance spectra of TiO<sub>2</sub> thin films on different substrates.

The refractive index can be determined by reflectance data using the following relation [27].

$$n = \sqrt{\frac{1 + \sqrt{R}}{1 - \sqrt{R}}}$$

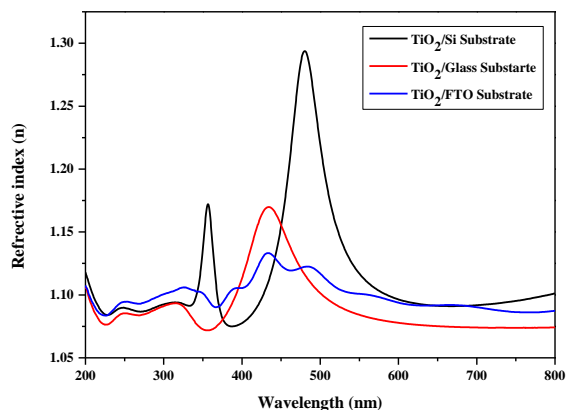


Fig. 5. Plot of refractive index as a function of wavelength of  $\text{TiO}_2$  thin films on different substrate.

The refractive index ( $n$ ) of  $\text{TiO}_2$  thin films on different substrates as the function of wave length is shown in Fig. 5, which show the oscillatory behavior of the refractive index in visible regions. The maximum values of refractive index are measured 1.3, 1.17 and 1.13 for Si,

Table 2. Optical results of  $\text{TiO}_2$  thin films on different substrates.

$\text{TiO}_2$ thin films	Peak 1		Peak 2		Energy Band gap (eV)	Max. Refractive index
	Position	Intensity (a.u)	Position	Intensity (a.u)		
Si	409.22	3.43	-	-	3.135	1.31
Glass	408.68	12.62	420.39	7.08	3.143	1.27
FTO	409.034	37.48	420.76	19.17	3.138	1.25

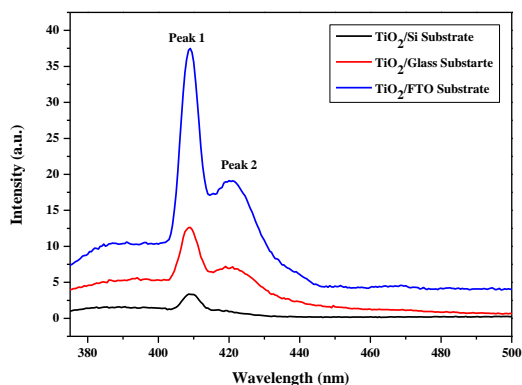


Fig. 6. Photoluminescence spectra of  $\text{TiO}_2$  thin films on different substrates.

#### 4. Conclusions

In this work, Titanium dioxide ( $\text{TiO}_2$ ) thin films were prepared by atomic layer deposition (ALD). The peaks in

glass and FTO substrate respectively. The values of refractive index are changing with substrate due to the roughness of thin films.

To study the defects in the  $\text{TiO}_2$  thin films by atomic layer deposition on different substrate was characterized by measuring the room-temperature photoluminescence (PL) spectra for excitation wavelength of 325nm. As it was shown in Fig. 6, two PL peaks at around 409 nm and 420 were observed from the  $\text{TiO}_2$  thin films. Peak 1 exhibited the band gap peak, which is slightly shifted with changing the substrate. This may be due to band recombination. Thus the free electrons excited in the conduction band recombine with the free holes in the valance band. The optical band gaps of  $\text{TiO}_2$  thin films samples were calculated using peak 1 position and given in table 2. The peak 2 only in glass and FTO substrate sample can be attributed to the excitonic PL peaks trapped by the surface states and defects [28] due to the oxygen vacancies [29-32]. The peak position and intensity of peak 2 is changed with changing the substrate of  $\text{TiO}_2$  thin films.

the spectra of  $\text{TiO}_2$  thin films deposited on Si, glass and FTO substrates confirm the mixed anatase and rutile structure and the other peaks arise from the substrates. It was observed from XRD analysis that the crystallite size calculated by anatase peak is higher as compared to the rutile peaks for each substrate. The maximum value of refractive index is measured 1.3, 1.17 and 1.13 for Si, glass and FTO substrate respectively. Two PL peaks at around 409 nm and 420 were observed from the  $\text{TiO}_2$  thin films. One exhibited the optical band gap peak, which is slightly shifted with changing the substrate. The second peak is only in glass and FTO substrate samples and can be attributed to the excitonic PL peaks trapped by the surface states and defects due to the oxygen vacancies. On the basis of our finding results about structural and optical parameters of  $\text{TiO}_2$  thin films, different substrate can be use in different nano and optoelectronic advance applications according to our requirements.

#### Acknowledgment

The authors would like to extend their sincere appreciation to the Deanship of Scientific Research at

King Saud University for its funding of this research through the Research Group Project No. RGP -1436-019.

## References

- [1] J. Chunyan, L. Ben, L. Zhongxiang, S. Jiaming Nanoscale Research Letters 2-9 (2015).
- [2] M. Leskelä, M. Ritala, Thin Solid Films **409**, 138 (2002).
- [3] V. Pore, Atomic Layer Deposition and Photocatalytic Properties of Titanium Dioxide Thin Films. Ph.D. Thesis, Helsinki University, Helsinki, Finland, 2010.
- [4] P. Liao, E. Carter, A. Chem. Soc. Rev. **42**, 2401 (2013).
- [5] Z. Li, W. Luo, M. Zhang, J. Feng, Z. Zou, Energy Environ. Sci. **6**, 347 (2013).
- [6] H. Tang, K. Prasad, R. Sanjinès, P.E. Schmid, Lévy F, J. Appl. Phys. **75**, 2042 (1994).
- [7] S. Chao, W.H. Wang, C.C.Lee, Appl Opt. **40**, 2117 (2001).
- [8] T. Yokogawa, S. Yoshii, A. Tsujimura, Y. Sasai, J. Merz, J. J. Appl. Phys. Part 2: Letters. **34**, L751 (1995).
- [9] H. Fukuda, S. Namioka, M. Miura, Y. Ishikawa, M. Yoshino, S. Nomura, J. J. Appl. Phys. **38**, 6034 (1999).
- [10] A. C. Stephen, X. C. Wang, M. T. Hsieh, H. S. Kim, W. L. Gladfelter, J. H. Yan, IEEE Trans Electron Devices **44**, 104 (1997).
- [11] A. Fujishima, K. Honda, Nature **238**, 37 (1972).
- [12] B. O'Regan, M. Gratzel, Nature **353**, 737 (1991).
- [13] A. Mills, R.H. Davies, D. Worsley, Chem Soc Rev. **22**, 417 (1993).
- [14] P. C. Maness, S. Smolinski, D. M. Blake, Z. Huang, E. J. Wolfrum, W.A. Jacoby, Appl Environ Microbiol. **65**, 4094 (1999).
- [15] Y. Paz, Z. Luo, L. Rabenberg, A. Heller, Mater. Res. Soc. **10**, 11 (1995).
- [16] I. Poullos, P. Spathis, A. Grigoriadou, K. Delidou, P. Tsooumparis, J. Environ Sci Health Part A **34**, 1455 (1999).
- [17] R. Cai, K. Hashimoto, K. Itoh, Y. Kubota, A. Fujishima, Chem Soc Japan **64**, 4 (1991).
- [18] M. A. Lazar, S. Varghese, S. S. Nair, Catalysts. **2**, 572 (2012).
- [19] H. Sakai, R. Baba, K. Hashimoto, Y. Kubota, A. Fujishima, Chem Lett. **24**, 185 (1995).
- [20] P. K. Dutta, A. Ginwalla, B. Hogg, B. R. Patton, B. Chwieroth, Z. Liang, J. Phys. Chem. B **103**, 4412 (1999).
- [21] Y. Xu, K. Yao, X. Zhou, Q. Cao, Sens Actuators B **14**, 492 (1993).
- [22] T. Won, S. Yoon, H.J. Kim, Electrochem. Soc. **139**, 3284 (1992).
- [23] X. Chen, W. Guan, G. Fang, X. Z. Zhao, Applied Surface Science **252**(5), 1561 (2005).
- [24] Ovid' Ko, Rev.Adv.Mater.Sci. **1**, 61 (2000).
- [25] R. Ferro, J.A. Rodriguez, A. Vigil, Mater.Sci.Eng. B **87**, 83 (2001).
- [26] X. S. Wang, Z. C. Wu, J. F. Webb, Z. G. Liu, Applied Physics A **77**, 561 (2003).
- [27] S. A. Mansoor, M. Jan, T. H. Syed, A. B. Shahzad, M. Ashraf, U. R. Naeem, J Mater Sci: Mater Electron **24**, 2432 (2013).
- [28] L.Q. Jing, Y.C. Qu, P.Q. Wang, Sol. Energy. Mater. Sol. C **90**, 295 (2006).
- [29] Y.Y. Peng, T.E. Hsieh, C.H. Hsu, Nanotechnology **17**, 174 (2006).
- [30] H.C. Ong, G.T. Du, J.Cryst. Growth. **265**, 471 (2004).
- [31] F. K. Shan, G. X. Liu, W. J. Lee, G. H. Lee, I. S. Kim, B. C. Shin, Appl. Phys. Lett. **86**, 221910 (2005).

\*Corresponding author: mansoor\_phys@yahoo.com